Molecular dynamics study of the repulsive form influence of the interaction potential on structural, thermodynamic, interfacial and transport properties.

Guillaume Galliero, Christian Boned

Molecular dynamics study of the repulsive form influence of the interaction potential on structural, thermodynamic, interfacial and transport properties.

Guillaume Galliero*, Christian Boned

Laboratoire des Fluides Complexes (UMR-5150), Université de Pau et des Pays de l'Adour,

BP 1155, F-64013 PAU Cedex, France

*Corresponding author: email: guillaume.galliero@univ-pau.fr;

Tel: +33 5 59 40 7704; Fax: +33 5 59 40 7695

Abstract

In this work, using extensive molecular dynamics simulations of several thermophysical properties, it is proposed to analyze possible relationships (in the corresponding states sense) between monoatomic fluids for which the repulsive interactions are modeled by an inverse *n*-power form, the Lennard-Jones 12-6 (LJ), or by an exponential one, the exponential-6 (Exp-6). To compare results between them, two possible definitions of Exp-6 potentials "equivalent" to the LJ one are proposed. In pure fluids, for a large range of thermodynamic conditions, the properties computed are the surface tension, liquid/vapour equilibrium densities, one-phase potential energy, pressure, isometric heat capacity, thermal pressure coefficient and self-diffusion, shear viscosity, thermal conductivity. Additionally, thermodiffusion (Soret effect) has been considered in "isotopic" equimolar mixtures. It is shown that, despites similarities exhibited by alike radial distribution functions, differences exist between the thermodynamic properties values provided by the LJ fluid and the two "equivalent" Exp-6 fluids. Nevertheless, quite surprisingly, when temperature and density are used as inputs, all three direct transport properties are shown to be nearly independent of the

choice of the potential tested. Unexpectedly, these similarities hold even for thermodiffusion which is *a priori* very sensitive to the nature of the interactions. These results indicate that the use of an Exp-6 potential form to describe non bonded/non polar interaction in molecular simulation is an alternative (more physically acceptable) to the LJ potential when dealing simultaneously with thermodynamic and transport properties. However, when only transport properties are considered (including thermodiffusion), the Exp-6 potential form should not lead to any differences compared to the LJ one.

1. Introduction

When performing classical molecular simulations of fluid thermophysical properties, the major issue concerns the choice of efficient, but simple, analytical inter and intra molecular potential forms in order to accurately describe the structure and the dynamic of dense fluids. In this context, the non bonded/non polar interactions (repulsion and van der Waals dispersion) are usually modelled with an effective pair potential, the Lennard-Jones 12-6 (LJ) one. When used on simple fluids (e.g. Argon), this two parameters potential mimics most of the features experimentally found in fluid states, despite its simplicity compared to quasi-exact potentials[1]. However, it represents the decay of the repulsive interaction by an inverse twelve-power dependence on intermolecular separation, which was chosen mainly for mathematical convenience and has no physical soundness[2]. Such an intrinsic weakness may be of importance because the structural properties of a simple fluid are principally determined by the intermolecular short-range repulsive interactions[3-4] as implicitly postulated by the widely used perturbation scheme.

One alternative to the LJ potential is the use of a variable repulsive exponent (Mie *n*-6 potential), but the problem of an inverse *n*-power formulation remains. The Exponential-6 (Exp-6) potential family provides a more physically based alternative[5] to describe the repulsion interaction (through an exponential form). This analytic form of the interaction potential has shown to be suitable to deal with very dense systems like those encountered in shock waves studies[6]. However, when performing molecular simulations, far less attention has been paid to the Exp-6 ones compared to the classical LJ and Mie *n*-6 potentials. This lack is especially obvious when dealing with transport properties. Nevertheless, it should be mentioned that interesting molecular simulations results on the Exp-6 potential family have been found recently[7-13], in particular in order to develop Equation of States (EoS)[14]. In the

following, by LJ or Exp-6 fluids, we mean monoatomic fluids where interactions are described by LJ or Exp-6 potentials respectively.

Using extensive molecular dynamics (MD) simulations on simple monoatomic fluids, it is proposed in this paper to quantify the differences on the values of some thermophysical (static and dynamic) properties computed for a fluid where the repulsion is described by an inverse n-power (the LJ one, n=12) and two "equivalent" fluids where the repulsion is described by an exponential formulation. In other words, it is analysed to which extent a corresponding states scheme (for each property) may exist between the LJ and the Exp-6 fluids. By doing so, the aim is to clarify for which thermophysical properties the Exp-6 potential, which is a more physically acceptable potential form than the inverse n- power one, could be an alternative to the LJ potential for describing non-polar/non bonded interactions of real fluids in molecular simulations. The thermodynamic conditions considered range from moderate to dense states for subcritical and supercritical temperatures (up to two times the critical one). The quantities computed are radial distribution functions, interfacial properties (equilibrium densities and surface tension), thermodynamic properties (potential energy, pressure, isometric heat capacity and thermal pressure coefficient) and transport properties (self-diffusion, shear viscosity, thermal conductivity and thermodiffusion in simple mixture).

In a first part, the LJ and Exp-6 interaction potentials are described together with the way the two "equivalent" Exp-6 potentials are defined. Then, the MD methods (as well as some technical details) used to estimate the various thermophysical properties are provided. Finally, all the results obtained on structural, interfacial, one-phase thermodynamic and transport properties are discussed. A particular emphasis is put on the thermodiffusion (Soret effect[15]) results, this transport property being the most interesting from the interactions (and so the potential shape) point of view[16-17].

2. Theory

2.1. Interaction potentials

In this work, two different kinds of effective truncated potentials have been used to describe interactions between particles, the Lennard-Jones 12-6 and the Exponential-6 potentials, which can be written respectively as:

$$U_{LJ} = \varepsilon\left[\left(\frac{r_m}{r}\right)^{12} - 2\left(\frac{r_m}{r}\right)^{6}\right] \tag{1}$$

$$U_{Exp-6} = \varepsilon\left[\left(\frac{6}{\alpha-6}\right)e^{-\alpha\left(\frac{r}{r_m}-1\right)} - \left(\frac{\alpha}{\alpha-6}\right)\left(\frac{r_m}{r}\right)^{6}\right] \tag{2}$$

where ε is the potential strength, r_m the distance at which the potential is minimum, α the stiffness of the repulsive slope and r the intermolecular separation. Usually, the Lennard-Jones 12-6 potential is rewritten in terms of, σ, the "atomic diameter", which is the distance at which the potential is null:

$$U_{LJ} = 4\varepsilon\left[\left(\frac{\sigma}{r}\right)^{12} - \left(\frac{\sigma}{r}\right)^{6}\right] \tag{3}$$

For both potential families a cutoff radius equal to $3.15r_m$ ($\approx 3.5\sigma$ for the LJ potential) has been applied during simulations.

2.2. Relationships between the potentials

In order to define an Exp-6 potential "equivalent" to the LJ one, different alternatives can be chosen. As previously done in the work of Lim[18], one way to find a relationship between both potentials (i.e. find the appropriate α in eq. (2)) is to equate their values, slopes and curvatures at the equilibrium distance, r_m:

$$\left(U_{Exp-6}\right)_{r=r_m} = \left(U_{LJ}\right)_{r=r_m} \tag{4}$$

$$\left(\frac{\partial U_{Exp-6}}{\partial r}\right)_{r=r_m} = \left(\frac{\partial U_{LJ}}{\partial r}\right)_{r=r_m} \tag{5}$$

$$\left(\frac{\partial^2 U_{Exp-6}}{\partial r^2}\right)_{r=r_m} = \left(\frac{\partial^2 U_{LJ}}{\partial r^2}\right)_{r=r_m} \tag{6}$$

By definition, eq. (5) is fulfilled as long as, at the equilibrium distance (the position of the minimum of the potential), the slopes of both potential functions are zero. The two other relations, eqs. (4,6), combined with the definition of both potentials, eqs. (1-2), lead to the following relation on α:

$$\alpha^2 - 19\alpha + 72 = 0 \tag{7}$$

As α should be greater than 6, the only physically acceptable solution is:

$$\alpha = \frac{19 + \sqrt{73}}{2} \approx 13.772 \tag{8}$$

Another way to define an Exp-6 potential "equivalent" to the LJ one (eq. (5) being always respected) is to impose that their values are equal at the equilibrium distance, eq. (4), and at the distance, σ, for which the potential is equal to zero :

$$\left(U_{Exp-6}\right)_{r=\sigma} = \left(U_{LJ}\right)_{r=\sigma} \tag{9}$$

Using the fact that for a LJ potential $r_m = 2^{1/6}\sigma$, eqs. (4, 9) lead to:

$$\alpha \approx 14.338 \tag{10}$$

In the following, the exponential 13.772-6 potential is noted Exp1 and the exponential 14.338-6 one is noted Exp2. Differences versus distance between Exp1 (or Exp2) and LJ potentials as well as between Exp2 and Exp1 potentials are shown on Fig. 1. It is interesting to note that, at short distances, both Exp-6 potentials are less repulsive (i.e. they are softer) than the LJ potential.

2.3. Molecular Dynamics simulations

In order to compare results provided by the Exp1, Exp2 and LJ fluids, a homemade molecular dynamics code[13] has been used. For sake of simplicity, all properties have been expressed in reduced units, using ε as the energy scale, σ as the length one and m, the molecular weight, as the mass one. They are noted with a star as superscript.

2.3.1. Radial distribution function and thermodynamic properties

The radial distribution function (RDF), $g(r)$, in a homogenous system, is computed thanks to[1]:

$$g(r) = \frac{V}{N^2}\left\langle \sum_{i=1}^{N}\sum_{j<i}^{N} \delta\left[\mathbf{r} - \mathbf{r}_{ij}\right] \right\rangle \tag{11}$$

where N is the number of particles, V the volume and $\mathbf{r}_{ij}$ the vector between centers of particles i and j. This quantity is of primary importance to analyze the structural correlations in a fluid[1,19].

In one-phase systems, the usual static properties are computed: density, ρ^*, temperature, T^*, potential energy, U_{pot}^* and the pressure P^*. Concerning U_{pot}^* and P^* in one phase systems, long-range corrections[1] are taken into account. In addition to these static properties, two second derivative thermodynamic properties have been computed[19], the isometric heat capacity, C_v^*, and the thermal pressure coefficient, γ_v^*:

$$C_V^* = \left[N - NT^* \left(\frac{3N}{2} - 1 \right) \left\langle E_k^{*-1} \right\rangle \right]^{-1} \tag{12}$$

$$\gamma_v^* = \frac{2C_v^*}{3}\left[\rho^* - \frac{\left\langle \delta E_k^* \delta P^* \right\rangle}{T^{*2}} \right] \tag{13}$$

where E_k is the kinetic energy and

$$\left\langle \delta E_k^* \delta P^* \right\rangle = \left\langle \left(E_k^* - \left\langle E_k^* \right\rangle \right)\left(P^* - \left\langle P^* \right\rangle \right) \right\rangle \tag{14}$$

In addition, the surface tension has been estimated along the liquid vapor coexistence line during diphasic simulations using the classical mechanical route[20]:

$$\gamma^* = \int_{-\infty}^{+\infty} \left[P_N^*(z^*) - P_T^*(z^*) \right] dz^* \qquad (15)$$

where $P_N^*(z^*)$ and $P_T^*(z^*)$ are respectively (relatively to the interface) the normal and tangential components of the pressure at the position z^*.

It is well known that the use of a truncated potential (as done in this work with a cutoff radius equal to $3.15r_m$) affects the amplitude of the surface tension computed and the equilibrium densities [21-22]. The way to introduce long range corrections in such inhomogeneous systems is still disputed[22]. In this work, long range corrections that influence the properties of the diphasic systems do not have been introduced because only relative deviations between results provided by LJ and Exp1/Exp2 fluids (with the same cutoff radius) are considered.

2.3.2. Transport properties

The first transport property that has been estimated in this work is the mass self-diffusion, D^*. To do so, the Einstein route[19] has been used during equilibrium molecular dynamics simulations:

$$D^* = \lim_{t \to \infty} \frac{1}{6Nt^*} \sum_{i=1}^{N} \left\langle \left[\mathbf{r}_\mathbf{i}^*(t^*) - \mathbf{r}_\mathbf{i}^*(0) \right]^2 \right\rangle \qquad (16)$$

where t^* is the time and $\mathbf{r}^*_i$ the position vector of particle i.

To compute the other transport properties, i.e. the shear viscosity, η^*, the thermal conductivity, λ^*, and the thermal diffusion factor, α_T, a boundary driven nonequilibrium molecular dynamics scheme proposed by Müller-Plathe[23] has been used.

For η^*, it consists in imposing a biperiodical flux of transverse linear momentum. To do so, the simulation box is divided into N_s slabs, then the two particles located respectively

in slab 1 and N_s with the highest momentum along the desired direction are exchanged with the two ones located in slab $N_s/2$ and $N_s/2+1$ which have the lowest momentum. Concerning λ^* the procedure is similar, but the biperiodical heat flux is induced by an exchange of kinetic energy. This procedure keeps constant the overall energy and momentum and corresponds simply to a redistribution in the simulation box of a certain amount of momentum for viscosity and kinetic energy for thermal conductivity. This exchange is done every A time steps (exchange/swap frequency) to avoid too large gradients and a non linear response. Once this boundary driven nonequilibrium molecular dynamics scheme is applied, after a transient state, a biperiodical gradient of transverse linear momentum for viscosity and of temperature for thermal conductivity will establish. Then, the property of interest is simply deduced from the Newton's law for viscosity and Fourier's law for thermal conductivity[24].

Concerning thermodiffusion in mixtures (the so called Soret effect in condensed phase which couples mass flux and thermal gradient[15]), the procedure is similar to the one for thermal conductivity[25], i.e. imposition of a biperiodical heat flux using the procedure described previously. First, the biperiodical thermal gradient will establish, then after a longer duration a biperiodical concentration gradient, due to thermodiffusion, will take place in the simulation box. This enables to determine the thermal diffusion factor[15] which writes for a binary mixture:

$$\alpha_T = -\frac{T}{x_1(1-x_1)}\frac{\nabla x_1}{\nabla T} \qquad (17)$$

where x_1 is the molar fraction of the first species of the mixture.

2.3.3. Simulation details

Classical periodic boundary conditions combined with a Verlet neighbors list have been applied. A reduced timestep, h^*, equal to 0.002 has been employed. To integrate the equation of motion, the velocity Verlet algorithm is used[1]. To maintain the desired

temperature during simulations, a Berendsen[26] thermostat with a large time constant equal to $1000h^*$ has been utilized. In order to estimate errors on the variables computed, the subblocks average method has been applied[1].

For simulations in one-phase fluid, a cubic simulation box containing 1500 particles has been employed. To obtain thermodynamic properties, runs of 2 10^6 timesteps have been used to collect data. Concerning transport properties, after discarding the transient states, data have been collected during between 3 and 10 10^6 timesteps to ensure a sufficient statistic. For viscosity, an exchange period, A, equal to 300 timesteps has been used, whereas for thermal conductivity and thermal diffusion this swap period was varying from 60 to 300 timesteps depending on the thermodynamic state in order to ensure a linear response[27-28].

For simulations involving a vapor-liquid interface, a non-cubic simulation box composed of 1500 to 2000 particles has been employed. In order to construct the initial system (which contains a planar liquid slab surrounded by its vapor), the procedure described in Ref. [29] has been used. To compute surface tension and vapor/liquid densities along the coexistence line, data have been collected during 5 10^5 timesteps.

Using these parameters, the uncertainty on the values is below 1 % for pressure, around 2 % for isometric heat capacity, 3% for mass diffusion and thermal pressure coefficient, 4% for viscosity and thermal conductivity, 5 % for surface tension and 10 % for thermal diffusion, see Appendix I-IV.

3. Results

3.1. Radial distribution function

The first quantity computed is the RDF of the LJ, Exp1 and Exp2 fluids for two dense states: ρ^*=0.9, T^*=1.0 (subcritical) and ρ^*=0.9, T^*= 2.5 (supercritical). As the results are nearly undistinguishable between LJ, Exp1 and Exp2 fluids, only the LJ RDF, see Fig. 2, and

the differences between the LJ RDF and the Exp1 and Exp2 ones, see Fig. 3, are shown for the two states.

As expected for such dense states, the fluid is highly structured especially for the lowest temperature system, see Fig. 2. In addition, there exists not only a strong first shell but also secondary and even ternary peaks indicating a long range structure. Concerning the differences between RDF obtained for the Exp-6 and LJ fluids, results shown in Fig. 3 (relatively to those given in Fig. 2) clearly indicate that the structure of these fluids are very similar especially for the lowest temperature and between Exp2 and LJ fluids. More precisely, the differences mainly occur at short distance in the first shell. In fact, it appears, see Fig. 3, that the Exp-6 RDF are larger than the LJ one for the shortest distance. This result is consistent with the fact that both Exp-6 potentials are less repulsive than the LJ one, see Fig. 1.

3.2. Interfacial properties

For the three fluids tested (LJ, Exp1 and Exp2) and for five different temperatures (T^*=0.7-1.1 with a step of 0.1), the vapor-liquid equilibrium densities, ρ_v^* and ρ_l^*, together with the associated surface tension, γ^*, have been computed. All simulation data are provided in Appendix I. It should be noted here that the interfacial properties obtained for the LJ fluid exhibit some deviations compared to those provided by other techniques[22,30]. These deviations are present on the whole temperature range and not only close to the critical point (where finite size effects become large). Nevertheless, as mentioned in section 2.4, this is mainly due to the use of a truncated potential (with a rather small cutoff radius equal to $3.15r_m$) without long range corrections. Notice that our results are in excellent agreement with those provided by Dunikov et al.[21] which provide values for a LJ truncated potential (at $3.5\sigma \approx 3.14r_m$) without long range corrections. They found that at T^*=0.9, γ^*=0.472, ρ_v^*=0.0218, ρ_l^*=0.725 and at T^*=1, γ^*=0.291, ρ_v^*=0.0432, ρ_l^*=0.665 whereas we obtained respectively,

γ^*=0.47±0.02, ρ_v^*=0.0217±0.005, ρ_l^*=0.725±0.003 and γ^*=0.29±0.03, ρ_v^*=0.041±0.004, ρ_l^*=0.667±0.004. In addition, apart from finite size effects that may occur, the cutoff radius employed (without long range corrections) implies an underestimation of the critical temperature[21], if this temperature is extrapolated from the results of the surface tension using a classical scaling law[20].

Concerning the densities along the coexistence line, Fig. 4 shows that both definitions of the Exp-6 potential "equivalent" to the LJ one provide results quite similar to the LJ ones with deviations increasing with temperature. More precisely, Exp-6 vapor densities are larger than LJ ones whereas Exp-6 liquid densities are smaller than LJ ones. In addition, the Exp1 fluid yields results closer to those of the LJ fluid than the Exp2 fluid especially in the liquid phase, see Table I and Fig. 4.

Concerning surface tension, see Fig. 5 and Table I, γ*values provided by all three fluids are close to each other but those yielded by the Exp2 fluid are always lower than the Exp1 ones which are lower than the LJ ones. Considering that γ* in such simple fluids follows a classical scaling law behavior[20], these results indicate that the critical temperature of the LJ fluid should be the highest among the three and that the critical temperature of the Exp 2 fluid is the lowest one (for the system studied). It is satisfying to notice that this is consistent with the work of Panagiotopoulos[31] which (using Grand canonical histogram reweighting Monte Carlo calculations) estimated that the LJ fluid critical temperature equals to 1.299 whereas the Exp 14-6 fluid one equals to 1.253. Using a polynomial interpolation to fit the values given in ref. [31], it can be estimated that the critical temperature equals 1.268 for the Exp1 fluid and 1.235 for the Exp2 fluid.

3.3. One-Phase thermodynamic properties

In addition to the interfacial properties, various thermodynamic quantities (pressure, P^*, potential energy, U^*, isometric heat capacity, C_v^* and thermal pressure coefficient, γ_v^*)

have been computed for seven different thermodynamic states covering from supercritical gas to very dense liquid. These states are summarized in Table II (the critical point[31] is located at T_c^*=1.299, ρ_c^*=0.316 and P_c^*=0.123). It is worth to note that states 6 and 7 correspond to very dense states (states for which RDF have been computed, see section 3.1), the density being more than two times the critical one and the pressures being respectively roughly 30 and 90 times the critical one. All simulations data are provided in Appendix II.

Table III indicates that second derivative thermodynamic properties values (heat capacity and thermal pressure coefficient) provided by both Exp1 and Exp2 fluids are close to those of the LJ fluid, whereas larger deviations exist on pressure and potential energy values. It is interesting to note, see Fig. 6, that the deviations between Exp-6 and LJ fluids values of pressure and potential energy are not markedly higher in dense states (3-7) than in moderately dense ones (1-2). Such result is unexpected as long as dense states correspond to conditions where the repulsive part of the potential is of primarily importance.

Concerning second derivative thermodynamic properties, Fig. 7 indicates that, apart from the moderate densities conditions (ρ*=0.3, state 1 and 2), Exp1 and Exp2 fluids yield C_v^* values slightly higher than the LJ fluid ones and somewhat lower results for γ_v^*. In addition, it is worth to note that deviations are generally larger in dense states than in moderately dense ones.

All results obtained for thermodynamic properties (one-phase and interfacial) indicate that, on average, the Exp1 fluid yields values closer to the LJ fluid ones than the Exp2 fluid. Nevertheless, none of both Exp-6 fluids is able to reproduce accurately the thermodynamic behavior of the LJ fluid. This is interesting as it clearly demonstrates (see Figs. 6-7) that a perfect corresponding states scheme between the LJ and the Exp-6 fluids is not reachable when dealing with thermodynamic properties. It should be noted that this point has already been noticed in Ref. [13]. Hence, when used to predict real fluids thermodynamic properties

by molecular simulations, in cases where the LJ potential (or more generally the Mie *n*-6 potential family) reveals deficiencies, the choice of an Exp-6 potential form may be a physically acceptable alternative as shown by Errington et al.[8]. In addition, such a potential form may also be used to construct molecular based Equations of States[12,32-33] as done recently with success for the Mie *n*-6 potential[34,35].

3.4. Direct transport properties

Corresponding states approaches[36] are frequently employed to estimate thermodynamic properties of simple real fluids, but they can also apply, to a reasonable extent, to transport properties as well[37]. In fact, strictly speaking, if one assumes that a corresponding states law holds perfectly between two compounds, this should be verified both for thermodynamic and transport properties.

Thus, as previously done for thermodynamic properties, for the same thermodynamic states given in Table II, direct transport properties including self-diffusion, D^*, shear viscosity, η^*, and thermal conductivity, λ^*, have been computed using MD simulations for the LJ, Exp1 and Exp2 pure fluids. Results are provided in Appendix III.

Keeping in mind the intrinsic uncertainties on the MD values (see section 2.6), the first most striking result is that values yielded by Exp1 and even more Exp2 fluids are very close to those provided by the LJ fluid in all cases, see Fig. 8. The deviations are always smaller than 7.5 % for the Exp1 fluid and 3.5 % for the Exp2 one, see Table IV. This indicates that a corresponding states behavior exists between the Exp2 and the LJ fluids (not too close from the critical point) when restricted to transport properties and when temperature and densities are used as inputs.

Besides, see Fig. 8, the deviations on self-diffusion (slightly overestimated by Exp1 and Exp2 fluids compared to the LJ fluid values) and viscosity (slightly underestimated by Exp1 and Exp2 fluids) values are roughly symmetric compared to the zero line. Such a

behavior is consistent with the Stokes-Einstein equation which implies that the product between mass diffusion and viscosity is function only of temperature and of particle size[24] and seems to make sense even for non colloidal systems[38,39].

Concerning a possible link between results shown on Figs. 6 and 8 (i.e. a link between results on thermodynamic and transport properties), the situation is not simple. For instance, in state 6, for both Exp1 and Exp2 fluids, pressure and self-diffusion are slightly overestimated whereas viscosity is underestimated compared to LJ fluid values. This is contradictory to the fact that, in simple non polar dense fluids, mass diffusion decreases with pressure whereas viscosity increases. In fact, this clearly demonstrates that a simultaneous corresponding state between Exp-6 and LJ (or more generally Mie *n*-6) fluids, for both thermodynamic and transport properties is not reachable. This could be interesting in order to circumvent some of the difficulties encountered by molecular simulations (when the LJ potential is used to describe non bonded/non polar interaction) to reproduce both thermodynamic and transport properties[14,40] of real fluids with the same set of molecular parameters.

3.5. Thermodiffusion

Thermodiffusion is the less well understood and modeled transport property in fluid mixtures[16]. In addition, this transport process is considered to be the most sensitive to the interaction potential shape, at least in low density conditions[41]. Therefore, for the thermodynamic states indicated in Table II, the thermal diffusion factor, α_T, has been computed for the three fluids studied in this work. To limit the complexity of the problem, only ideal "isotopic" equimolar mixtures have been studied[42], i.e. equimolar mixtures for which r_m and ε are equal for both compounds. The compounds are only differentiated by their mass. We have employed m_2=10m_1 to obtain a sufficiently significant relative separation between the two species[42]. Simulation results are given in Appendix IV.

Unexpectedly, see Fig. 9, it appears that both Exp1 and Exp2 fluids are able to provide α_T values very close to those given by the LJ fluid: the Average Absolute Deviation (AAD) between Exp1 and LJ results is equal to 2.3 % and AAD between Exp2 and LJ results is equal to 1.9 %.

This behavior noted on α_T is interesting as it unambiguously shows that, as for direct properties, for a given set of T^* and ρ^*, thermal diffusion in "isotopic" mixtures is not largely affected by the choice of the shape of the repulsive part of the potential used to describe the interactions (at least between Exp-6 and LJ) in moderate to dense systems (ρ^*=0.3-0.9). Consequently, thermal diffusion (with the precision accessible by MD simulations at that time) cannot systematically be used to discriminate between potential shapes to describe non bonded/ non polar interactions as commonly believed. However, in more complex mixtures, this property can be a good molecular description probe as long as it has been shown that the description of other interactions is of primary importance on the amplitude and even the sign of thermodiffusion[17,39,43-44].

4. Conclusion

In this work, using extensive MD simulations, we have carried out a careful analysis of the similarities between fluids described by potentials where the repulsion is modeled by an inverse *n*-power repulsion or by an exponential one. This has been done by studying structure, interfacial, thermodynamic and transport properties (including thermodiffusion) of Lennard-Jones 12-6 and two "equivalent" Exp-6 fluids (using two different definitions of what means "equivalent"), for a large range of thermodynamic conditions.

Despites similarities reflected by very similar radial distribution functions, it has been noted that no perfect corresponding states scheme could be established between Exp-6 and LJ fluids when dealing with both interfacial (equilibrium densities and surface tension) and one-phase thermodynamic properties (potential energy, pressure, isometric heat capacity and

thermal pressure coefficient). In addition, it has been shown that the values of these properties provided by the Exp1 fluid (α=13.772, the softer one), are generally closer to the LJ fluid ones than those provided by the Exp2 fluid (α=14.338).

Concerning direct transport properties in pure fluids (self-diffusion, shear viscosity and thermal conductivity), results for all the three fluids have been found to be very similar for a given set of T^* and ρ^*, even in very dense phases (ρ^*=0.9). This is particularly obvious between LJ and Exp2 fluids results, the deviations being always smaller than 3.5 %. Even more surprising, when analyzing the thermodiffusion (Soret effect) in "isotopic" mixtures (m_2/m_1=10), which is, *a priori*, a transport property very sensitive to the nature of the interactions, deviations between Exp-6 and LJ fluids results remain always small and within their respective error bars (below 3.6 % for all states studied between Exp2 and LJ fluids).

These results on transport properties, clearly demonstrates that, for the tested range of thermodynamic conditions and using T^* and ρ^* as inputs, a nearly perfect corresponding states law on transport properties (including thermodiffusion) exists between Exp-6 and LJ fluids (especially between Exp2 and LJ fluids). Nevertheless, a corresponding states scheme valid for all properties (static and dynamic, simultaneously) between these fluids is unreachable as the deviations between results for Exp-6 and LJ fluids for both thermodynamic and transport properties are not linked.

From these results, it can be deduced that the use of an exponential form of the repulsive part of the potential to describe non bonded/non polar interactions is an alternative (more physically acceptable) to the more usual inverse *n*-power formulation when used to predict simultaneously thermodynamic and transport properties of real dense fluids by molecular simulations. However, when only transport properties (including thermodiffusion) are involved and if T^* and ρ^* are used as inputs (for ρ^* up to 0.9), the Exp-6 potential form should not lead to any differences compared to the more usual LJ one.

Acknowledgements:

A part of this work, concerning thermodiffusion, has been performed under the Diffusion and Soret Coefficient project supported by ESA. We gratefully acknowledge computational facilities provided by TREFLE laboratory, which supercomputer has been financially supported by the Conseil Régional d'Aquitaine.

References

[1] M.P. Allen and D.J. Tildesley, *Computer simulations of liquids* (Oxford Science Publications, Oxford, 1987).

[2] I.G. Kaplan, *Intermolecular Interactions: Physical Picture, Computational Methods and Model Potentials* (John Wiley and Sons, New York, 2006).

[3] T. Young and H.C. Andersen, J. Phys. Chem. B **109**, 2985 (2005)

[4] I. Nezbeda, Mol. Phys. **103**, 59 (2005).

[5] M. Ross and F.H. Ree, J. Chem. Phys. **73**, 6146 (1980).

[6] W.J. Nellis, A.C. Mitchell, F.H. Ree, M. Ross, N.C. Holmes, R.J. Trainor and D.J. Erskine, J. Chem. Phys. **95**, 5268 (1991).

[7] H.L. Vörtler, I. Nezbeda and M. Lisal, Mol. Phys. **92**, 813 (1997).

[8] J.R. Errington and A. Z. Panagiotopoulos, J. Phys. Chem. B. **103**, 6314 (1999).

[9] G.W. Wu, R.J. Sadus, Fluid Phase Equilib. **170**, 269 (2000).

[10] S. Bastea, Phys. Rev. E **68**, 312041 (2003)

[11] H. Zhang and J. F. Ely, Fluid Phase Equilib., **217**, 111 (2004).

[12] G. Galliero, C. Boned, A. Baylaucq and F. Montel, Phys. Rev. E **73**, 061201 (2006).

[13] G. Galliero, C. Boned, A. Baylaucq and F. Montel, Chem. Phys. **333**, 219 (2007).

[14] J. Sun, Q. Wu, L. Cai, F. Jing, Chem. Phys. Letters **449**, 72 (2007).

[15] S.R. de Groot and P. Mazur, *Non-Equilibrium Thermodynamics* (Dover, 1984).

[16] S. Wiegand, J. Phys. Cond. Matter **16**, R357 (2004).

[17] P.A. Artola and B. Rousseau, Physical Review Letters **98**, 125901 (2007).

[18] T.C. Lim, J. Math. Chem. **33**, 279 (2003).

[19] J.M. Haile, *Molecular Dynamics simulation: Elementary methods* (John Wiley & Sons, New York, 1992).

[20] J.S. Rowlinson and B. Widom, *Molecular Theory of Capillarity* (Dover, New-York, 2002).

[21] D.O Dunikov, S.P. Malyshenko and V.V. Zhakhovskii, J. Chem. Phys. **115**, 6623 (2001).

[22] V.K. Shen, R.D. Mountain, J.R. Errington, J. Phys. Chem. B **111**, 6198 (2007).

[23] F. Müller-Plathe, Phys. Rev. E **59**, 4894 (1999).

[24] R.B. Bird, W.E. Stewart and E.N. Lightfoot, *Transport Phenomena* (John Wiley & Sons, New York, 2007).

[25] P. Bordat, D. Reith and F. Müller-Plathe, J. Chem. Phys. **115**, 8978 (2001).

[26] H.J.C Berendsen, J.P.M. Postma, W.F. van Gunsteren, A. di Nola and J.R. Haak, J. Chem. Phys. **81**, 3684 (1984).

[27] P. Bordat and F. Müller-Plathe, J. Chem. Phys. **116**, 3362 (2002).

[28] G. Galliero, C. Boned and A. Baylaucq, Ind. Eng. Chem. Res. **44**, 6963 (2005).

[29] D. Duque, J.C. Pàmies and L.F. Vega, J. Chem. Phys. **121**, 11395 (2004).

[30] J.J. Potoff and A.Z. Panagiotopoulos, J. Chem. Phys. **112**, 6411 (2000).

[31] A.Z. Panagiotopoulos, J. Chem. Phys. **112**, 7132 (2000).

[32] J. Kolafa and I. Nezbeda, Fluid Phase Equilib. **100**, 1 (1994).

[33] E.A. Müller and K.E. Gubbins, Ind. Eng. Chem. Res. **40**, 2193 (2001).

[34] T. Lafitte, D. Bessières, M.M. Pineiro and J.L. Daridon, J. Chem. Phys. **124**, 024509 (2006).

[35] G. Galliero, T. Lafitte, D. Bessieres and C. Boned, J. Chem. Phys. **127**, 184506 (2007).

[36] H.W. Xiang, *The Corresponding-States Principle and its Practice: Thermodynamic, Transport and Surface Properties of Fluids* (Elsevier, Amsterdam, 2005).

[37] B.E. Poling, J. M. Prausnitz and J.P. O'Connell, *The Properties of Gases and Liquids* (McGraw-Hill, New-York, 2001).

[38] D.M. Heyes, M.J. Nuevo, J.J. Morales and A.C. Branka, J. Phys. Cond. Matt. **10**, 10159 (1998).

[39] G. Galliero and S. Volz, J. Chem. Phys. **128**, 064505 (2008).

[40] E. Ruckenstein and H. Liu, Ind. Eng. Chem. Res. **36**, 1927 (1997).

[41] S. Chapman and T.G. Cowling, *The Mathematical Theory of Non-Uniform Gases,* Cambridge Mathematical Library, Cambridge, 1970.

[42] G. Galliero, M. Bugel and B. Duguay, Journal of NonEqui. Thermo. **32**, 251 (2007).

[43] C. Nieto-Draghi, J.B. Avalos and B. Rousseau, J. Chem. Phys. **122**, 1 (2005).

[44] J. Xu, S. Kjelstrup, D. Bedeaux and J.-M Simon, Phys. Chem. Chem. Phys. **9**, 969 (2007).

Appendix I:

Interfacial properties (equilibrium densities and surface tension) of the LJ, Exp1 and Exp2 fluids. Values in parenthesis represent the uncertainties on the last digit.

T*	LJ			Exp1			Exp2		
	ρ_v^*	ρ_l^*	γ^*	ρ_v^*	ρ_l^*	γ^*	ρ_v^*	ρ_l^*	γ^*
0.7	0.0032(11)	0.823(3)	0.90(4)	0.0038(12)	0.824(2)	0.84(3)	0.0045(5)	0.813(3)	0.78(3)
0.8	0.009(13)	0.776(2)	0.69(2)	0.0105(16)	0.776(3)	0.64(3)	0.0130(8)	0.762(3)	0.61(2)
0.9	0.0217(15)	0.725(3)	0.47(2)	0.025(3)	0.723(2)	0.44(2)	0.028(2)	0.706(3)	0.39(3)
1	0.041(4)	0.667(4)	0.29(3)	0.051(4)	0.660(5)	0.27(3)	0.058(5)	0.641(4)	0.23(3)
1.1	0.086(5)	0.594(6)	0.15(4)	0.098(6)	0.581(8)	0.12(3)	0.113(5)	0.542(6)	0.08(4)

Appendix II:

One-phase thermodynamic properties (potential energy, pressure, isometric heat capacity and thermal pressure coefficient) of the LJ, Exp1 and Exp2 fluids. Values in parenthesis represent the uncertainties on the last digit.

State	LJ				Exp1				Exp2			
	U^*	P^*	C_v^*	γ_v^*	U^*	P^*	C_v^*	γ_v^*	U^*	P^*	C_v^*	γ_v^*
1	-2.066	0.225	1.94(2)	0.559(8)	-2.000	0.24	1.95(3)	0.560(9)	-1.947	0.255	1.93(5)	0.552(10)
2	-1.826	0.746	1.670(10)	0.512(5)	-1.750	0.756	1.680(10)	0.520(8)	-1.704	0.773	1.675(9)	0.510(6)
3	-4.039	4.38	2.000(9)	2.59(3)	-3.826	4.32	2.040(7)	2.526(15)	-3.746	4.443	2.038(6)	2.546(15)
4	-5.530	1.026	2.385(15)	4.82(7)	-5.357	1.111	2.45(4)	4.749(14)	-5.253	1.18	2.433(22)	4.76(9)
5	-4.407	7.16	2.158(10)	3.56(4)	-4.148	6.98	2.22(7)	3.49(7)	-4.067	7.17	2.208(14)	3.48(4)
6	-6.049	3.29	2.695(34)	6.71(17)	-5.840	3.37	2.81(4)	6.65(21)	-5.741	3.45	2.79(4)	6.70(18)
7	-4.580	11.63	2.360(13)	4.83(7)	-4.270	11.21	2.400(20)	4.52(8)	-4.193	11.51	2.414(17)	4.65(7)

Appendix III:

Direct transport properties (self-diffusion, viscosity and thermal conductivity) of the LJ, Exp1 and Exp2 fluids. Values in parenthesis represent the uncertainties on the last digit.

State	LJ			Exp1			Exp2		
	D*	η*	λ*	D*	η*	λ*	D*	η*	λ*
1	0.675(17)	0.315(10)	1.43(7)	0.663(21)	0.311(10)	1.42(9)	0.685(14)	0.312(16)	1.43(8)
2	0.995(20)	0.406(16)	1.73(9)	0.987(25)	0.406(16)	1.73(11)	0.993(19)	0.413(19)	1.75(10)
3	0.260(9)	1.25(4)	5.36(19)	0.276(5)	1.21(7)	5.17(25)	0.271(10)	1.23(9)	5.25(24)
4	0.068(2)	2.08(11)	6.12(24)	0.068(2)	2.02(8)	6.10(24)	0.067(2)	2.05(10)	6.13(22)
5	0.188(5)	1.78(10)	7.26(24)	0.198(4)	1.73(10)	7.05(30)	0.194(5)	1.765(61)	7.18(27)
6	0.036(1)	4.13(16)	8.43(32)	0.037(1)	3.90(17)	8.26(33)	0.036(1)	4.02(16)	8.41(37)
7	0.132(3)	2.77(9)	9.86(42)	0.139(3)	2.57(10)	9.41(38)	0.134(3)	2.67(23)	9.61(36)

Appendix IV:

Thermal diffusion factors in "isotopic" equimolar mixtures (m_2/m_1=10) for the LJ, Exp1 and Exp2 fluids. Values in parenthesis represent the uncertainties on the last digit.

State	α_T LJ	α_T Exp1	α_T Exp2
1	0.80(12)	0.80(15)	0.78(15)
2	0.91(10)	0.91(9)	0.93(10)
3	2.07(12)	2.04(18)	2.01(13)
4	2.36(14)	2.49(16)	2.40(29)
5	2.32(18)	2.29(20)	2.33(15)
6	2.34(29)	2.26(30)	2.35(31)
7	2.48(15)	2.44(13)	2.36(13)

Tables:

Table I: Interfacial properties Average Absolute Deviations (AAD), in percentage, compared to LJ results of both Exp1 and Exp2 potentials. Values in parenthesis represent the Maximum absolute Deviation.

	Vapor density	Liquid density	Surface tension
Exp1	18.1 (25.9)	0.7 (2.2)	9.9 (20)
Exp2	37.2 (44.4)	3.7 (8.8)	21.5 (43.3)

Table II: Thermodynamic states studied in the one-phase systems

State	1	2	3	4	5	6	7
ρ^*	0.3	0.3	0.7	0.8	0.8	0.9	0.9
T^*	1.5	2.5	2.5	1	2.5	1	2.5

Table III: Thermodynamic properties average absolute deviations (in percentage) compared to LJ results of both Exp1 and Exp2 potentials. Values in parenthesis represent the Maximum absolute Deviation.

	P^*	U_{tot}^*	C_v^*	γ_v^*
Exp1	3.7 (8.3)	4.6 (6.8)	2.1 (4.1)	2.2 (6.4)
Exp2	5.6 (15.0)	6.6 (8.4)	1.9 (3.6)	1.6 (3.9)

Table IV: Transport properties AAD (in percentage) compared to LJ results of both Exp1 and Exp2 potentials. Values in parenthesis represent the Maximum absolute Deviation.

	D^*	η^*	λ^*
Exp1	2.7 (5.3)	3.4 (7.3)	2.0 (4.5)
Exp2	1.3 (2.1)	1.8 (3.5)	1.0 (2.6)

Figure captions:

Figure 1: Left, differences between Exp1(continuous line) or Exp2(dashed line) and LJ potentials values versus the distance ($r^* = r/\sigma$ going from 0.95 to 3.5). Right, differences between Exp2 and Exp1 potentials values versus the distance.

Figure 2: RDF of the LJ fluid at ρ^*=0.9 and T^*=1 (full line) or T^*=2.5 (dashed line).

Figure 3: Differences between Exp1 (dashed lines) or Exp2 (full lines) RDF and LJ ones; left at ρ^*=0.9 and T^*=1 and right at ρ^*=0.9 and T^*=2.5.

Figure 4: Vapor (left part) and liquid (right part) densities along the coexistence line for various temperature and three different fluids, circles: LJ, triangles: Exp1 and squares: Exp2.

Figure 5: Surface tension versus temperature for three different fluids, circles: LJ, triangles: Exp1 and squares: Exp2

Figure 6: Deviations (in %) on pressure, circles, and potential energy, down triangles, between Exp1 (open symbols)/Exp 2 (full symbols) fluids results and LJ fluid ones for various thermodynamic states, see Table II.

Figure 7: Deviations (in %) on isometric heat capacity, circles, and thermal pressure coefficient, down triangles, between Exp1 (open symbols)/Exp 2 (full symbols) fluids results and LJ fluid ones for various thermodynamic states, see Table II.

Figure 8: Deviations (in %) on self-diffusion, circles, viscosity, squares, and thermal conductivity, down triangles, between Exp1 (open symbols)/Exp 2 (full symbols) fluids results and LJ fluid ones for various thermodynamic states, see Table II.

Figure 9: Thermal diffusion factor deviations (in %) between Exp1 (open circles)/Exp 2 (full circles) fluids results and LJ fluid ones for various thermodynamic states, see Table II.

Figure 1:

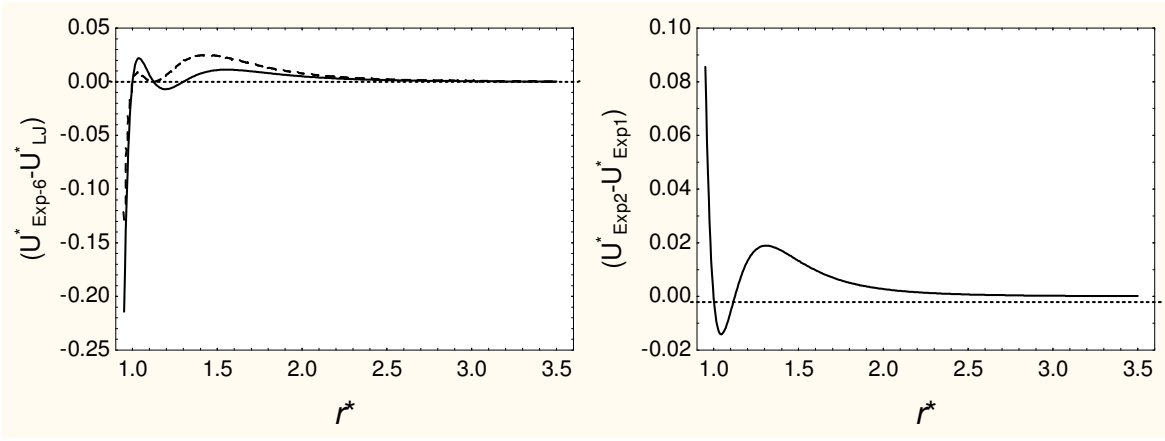
0.05
0.00
-0.05
-0.10
-0.15
-0.20
-0.25
1.0
1.5
2.0
2.5
3.0
3.5
r*
(U*Exp-6-U*LJ)
0.10
0.08
0.06
0.04
0.02
0.00
-0.02
1.0
1.5
2.0
2.5
3.0
3.5
r*
(U*Exp2-U*Exp1)

Figure 2:

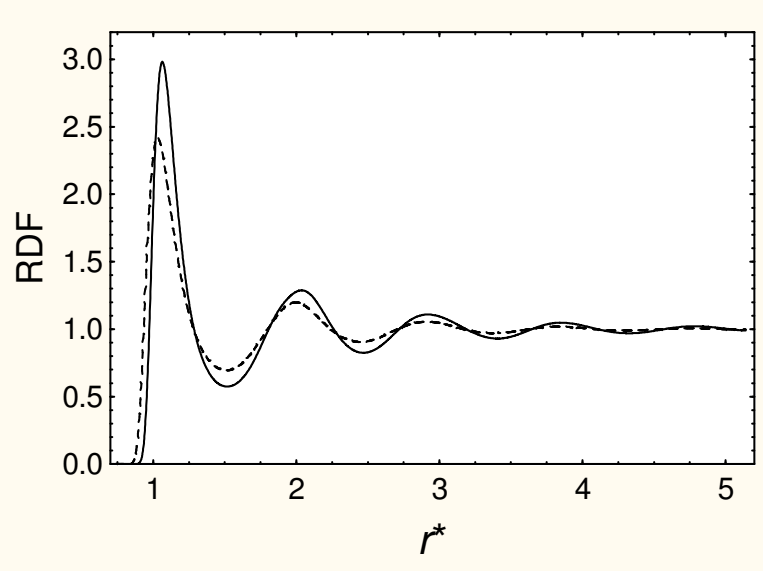

Figure 3:

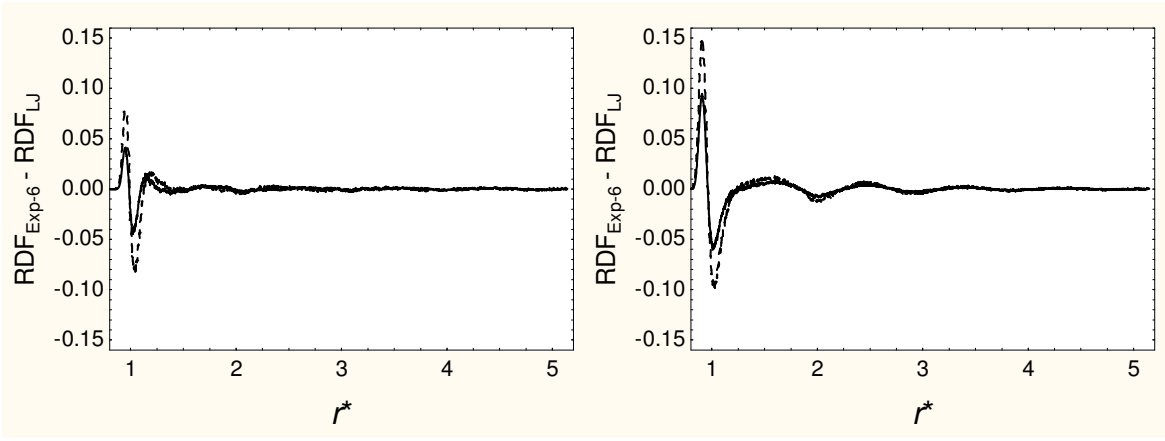
0.15
0.10
0.05
0.00
-0.05
-0.10
-0.15
RDF_Exp-6 - RDF_LJ
1
2
3
4
5
r*
0.15
0.10
0.05
0.00
-0.05
-0.10
-0.15
RDF_Exp-6 - RDF_LJ
1
2
3
4
5
r*

Figure 4:

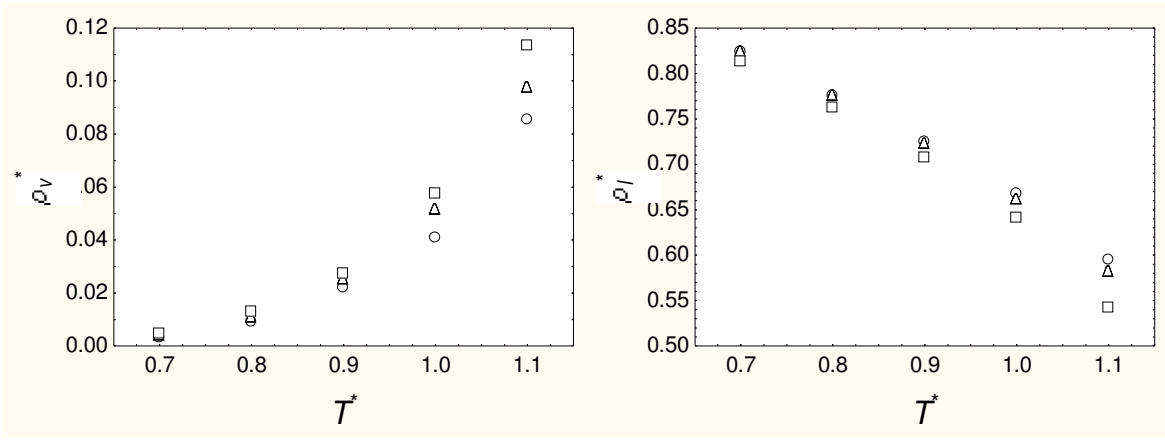
0.12
0.10
0.08
0.06
0.04
0.02
0.00
ρ_V^*
0.7
0.8
0.9
1.0
1.1
T^*
0.85
0.80
0.75
0.70
0.65
0.60
0.55
0.50
ρ_l^*
0.7
0.8
0.9
1.0
1.1
T^*

Figure 5:

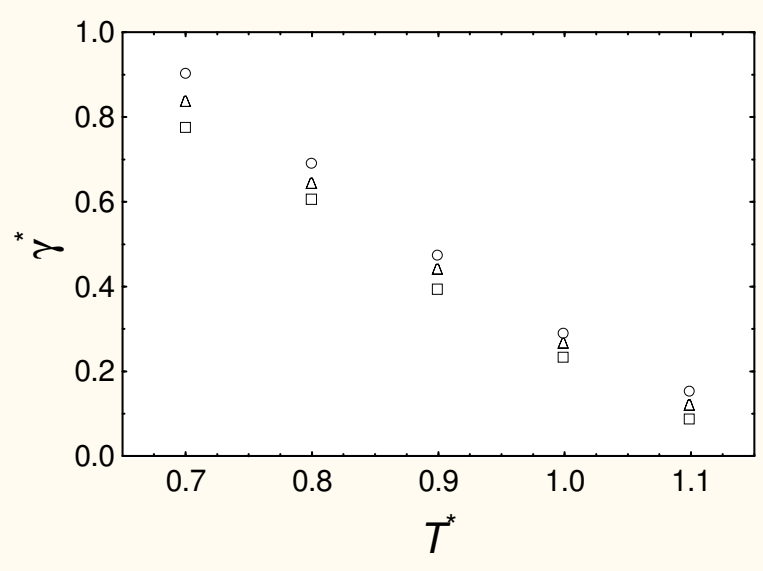

Figure 6:

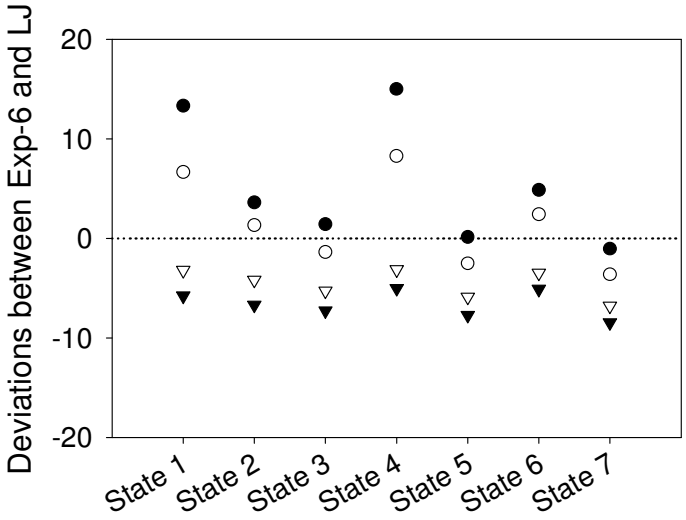
Deviations between Exp-6 and LJ
20
10
0
-10
-20
State 1
State 2
State 3
State 4
State 5
State 6
State 7

Figure 7:

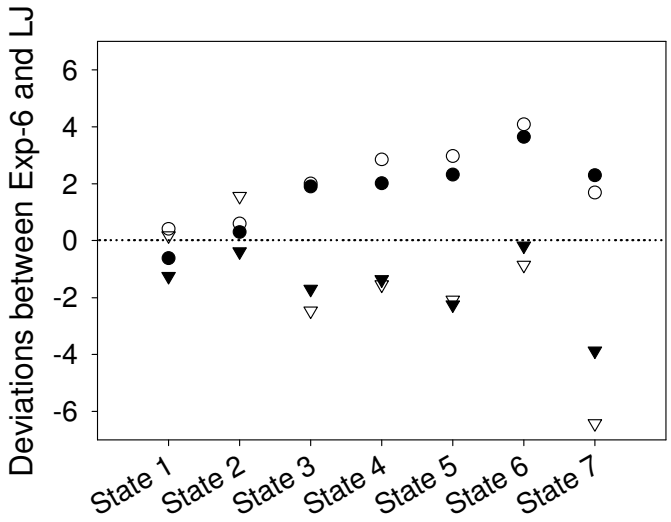
Deviations between Exp-6 and LJ
6
4
2
0
-2
-4
-6
State 1
State 2
State 3
State 4
State 5
State 6
State 7

Figure 8:

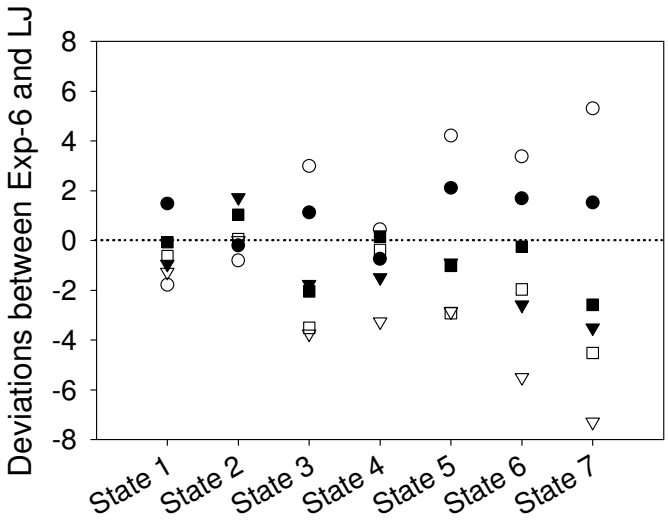
Deviations between Exp-6 and LJ
8
6
4
2
0
-2
-4
-6
-8
State 1
State 2
State 3
State 4
State 5
State 6
State 7

Figure 9:

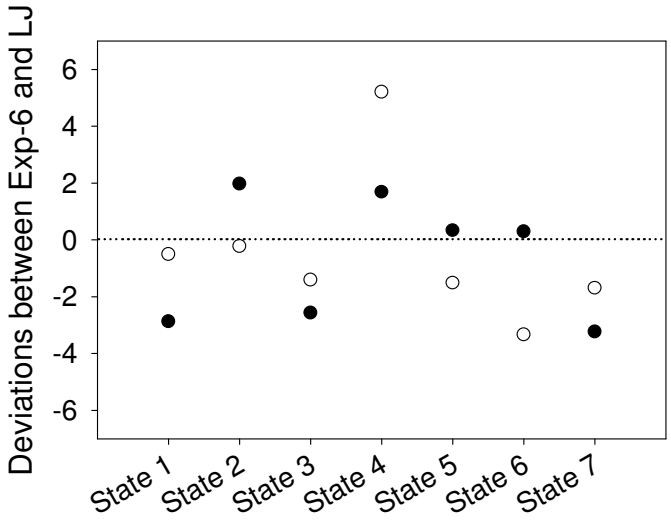
Deviations between Exp-6 and LJ
6
4
2
0
-2
-4
-6
State 1
State 2
State 3
State 4
State 5
State 6
State 7